RIVER RESEARCH AND APPLICATIONS

River. Res. Applic. **25**: 1071–1089 (2009)

Published online 21 November 2008 in Wiley InterScience
(www.interscience.wiley.com) DOI: 10.1002/rra.1207

REGIONALIZATION OF NATURAL FLOW REGIME: APPLICATION TO ENVIRONMENTAL FLOW OPTIMIZATION AT UNGAUGED SITES

JENQ-TZONG SHIAU[a] and FU-CHUN WU[b]*

[a]*Department of Hydraulic and Ocean Engineering, National Cheng Kung University, Tainan 701, Taiwan*
[b]*Department of Bioenvironmental Systems Engineering, Hydrotech Research Institute and Center for Ecological Engineering, National Taiwan University, Taipei 106, Taiwan*

ABSTRACT

In this work we use the regionalization approach (RA) to derive the natural flow regime at an ungauged site. The derived natural flow regime, expressed by the regional cdf models of 32 indicators of hydrologic alteration (IHA) is used in the histogram matching approach (HMA) to seek the optimal environmental flows for a proposed multiobjective diversion weir in Taiwan. The results reveal that the outcomes associated with the planning constant scheme are significantly improved by the optimal time-varying scheme. The histogram dissimilarities of 32 IHA associated with the planning scheme are consistently greater than those associated with the optimal scheme, especially for low-flow IHA. Despite the inherent discrepancy between different approaches to generating flow data at the ungauged site, the optimal outcomes resulting from the RA-based natural flow regime appear to be plausible and consistent with those reported in the previous work, thus validating the RA used in this work. We also explore the effect of weighting factors on the optimal outcomes. The results reveal that the weighting factor of the ecosystem needs objective dominates all optimal outcomes, while those of the agricultural demands and interbasin transfers objectives have minor effects on the optimal outcomes. The global optimal solution is obtained with a full or null weighting assigned to the ecosystem needs objective, while the least optimal solution is obtained as the interbasin transfers objective is given a null weighting and the agricultural demands objective is weighted more than the ecosystem needs objective. River managers and decision makers may select more balanced weir operation strategies based on the results presented in this work. Copyright © 2008 John Wiley & Sons, Ltd.

KEY WORDS: regionalization approach (RA); index flood method (IFM); indicators of hydrologic alteration (IHA); histogram matching approach (HMA)

Received 30 March 2008; Revised 21 July 2008; Accepted 18 September 2008

INTRODUCTION

Planning and development of water resources often demands one to cope with the problem of scarce data. For this reason, the International Association of Hydrological Sciences (IAHS) has promoted the prediction in ungauged basins (PUB) initiative for advancing hydrologic predictions in ungauged basins (Sivapalan, 2003). This same problem now increasingly receives attention from the river conservation/restoration community because establishment of management criteria and assessment of hydrologic impacts rely heavily on sufficient records of flow. For example, Richter *et al*. (1997) suggested that at least 20 years of daily flows are required for defining the natural ranges of flow variability. The reality, however, is that flow records in many project sites hardly meet this requirement.

A line of approaches to tackle such a problem is pooling at-site information within a hydrologically similar region and scaling the derived regional model to the ungauged sites. This has been conceptually described as 'trading space for time' (Hosking and Wallis, 1997). Thorough reviews of the regionalization approaches (RA) can be found in Cunnane (1988) and GREHYS (1996). Among the existing RA, the index flood method (IFM),

*Correspondence to: Fu-Chun Wu, Department of Bioenvironmental Systems Engineering, Hydrotech Research Institute and Center for Ecological Engineering, National Taiwan University, Taipei 106, Taiwan. E-mail: fcwu@ntu.edu.tw

Abbreviations: cdf, cumulative distribution function; GEV, generalized extreme-value distribution; GLO, generalized logistic distribution; GPA, generalized Pareto distribution; HMA, histogram matching approach; IAHS, international association of hydrological sciences; IFM, index flood method; IHA, indicators of hydrologic alteration; LN3, three-parameter lognormal distribution; PE3, pearson type III distribution; PUB, prediction in ungauged basins; RA, regionalization approach; RVA, range of variability approach

proposed by Dalrymple (1960), has become particularly popular for the flood/rainfall frequency analyses since Hosking and Wallis (1993) presented the *L*-moment-based measures for evaluating the fitness of the model. The IFM has been extensively adopted to derive the regional frequency distributions of extreme flood and rainfall and to determine the design flood and rainfall at ungauged sites (e.g. Madsen *et al*., 1997; Parida *et al*., 1998; Smithers and Schulze, 2001; Kjeldsen *et al*., 2002; Fowler and Kilsby, 2003; Lim and Lye, 2003; Zhang and Hall, 2004; Kumar and Chatterjee, 2005; Trefry *et al*., 2005; Atiem and Harmancioglu, 2006; Norbiato *et al*., 2007).

On the other hand, determination of environmental flows for sustaining the riverine ecosystems continues to be a challenge for contemporary scientists and decision makers. Over the last decade, the concept of 'natural flow regime' has been emerging as a paradigm for river conservation and restoration (Poff *et al*., 1997), which recognizes five components of flow regime (i.e. magnitude, duration, timing, frequency and rate of change) as the primary regulators of the ecological processes in rivers. Olden and Poff (2003) provided a review on over 200 hydrologic indices for characterizing natural and altered flow regimes. Among the many indices, Richter *et al*. (1996) adopted 32 hydrologic parameters to develop a suite of so-called indicators of hydrologic alteration (IHA) (see Table I). Each of the IHA is ecologically relevant when considering rivers in general. For a particular river, species, or period of time, however, some of the IHA may be more relevant than others. The IHA have become a popular tool for river research and management. For example, the authors have presented a series of work in which the IHA-based range of variability approach (RVA) and histogram matching approach (HMA) were used to define the natural flow regime and assess the hydrologic alterations induced by flow diversions (Shiau and Wu, 2004a,b, 2006, 2007a,b, 2008). For additional examples, the readers are referred to the 'IHA applications database' prepared by The Nature Conservancy (2005).

Table I. Indicators of hydrologic alteration (IHA) used in the HMA

IHA group	Hydrologic parameter (units)
Group 1: Magnitude of monthly flows	Mean flow of each calendar month (m^3/s)
Group 2: Magnitude and duration of annual extreme flows and base flow condition	Annual 1-day minimum flow (m^3/s)
	Annual 1-day maximum flow (m^3/s)
	Annual 3-day minimum flow (m^3/s)
	Annual 3-day maximum flow (m^3/s)
	Annual 7-day minimum flow (m^3/s)
	Annual 7-day maximum flow (m^3/s)
	Annual 30-day minimum flow (m^3/s)
	Annual 30-day maximum flow (m^3/s)
	Annual 90-day minimum flow (m^3/s)
	Annual 90-day maximum flow (m^3/s)
	Base flow condition (annual 7-day minimum flow divided by annual mean flow) (–)
Group 3: Timing of annual extreme flows	Julian date of annual 1-day minimum flow
	Julian date of annual 1-day maximum flow
Group 4: Frequency and duration of high and low pulses*	Number of high pulses in each year
	Number of low pulses in each year
	Mean duration of high pulse (days)
	Mean duration of low pulse (days)
Group 5: Rate and frequency of flow changes	Rise rate (mean of all positive differences between consecutive daily flows) ($m^3/s/day$)
	Fall rate (mean of all negative differences between consecutive daily flows) ($m^3/s/day$)
	Number of flow reversals

A total of 32 IHA are categorized by five groups of hydrologic features.
*High and low pulses are those periods in which the daily flows are above the 75th- and below the 25th-percentile pre-impact daily flows, respectively.

DOI: 10.1002/rra

Quantifying natural and altered flow regimes using the above IHA-based approaches would also require sufficient records of flow that are unavailable at many project sites. In this work we use the RA to derive the natural flow regime at an ungauged site, which is integrated with the HMA to seek the optimal environmental flow scheme for a proposed multiobjective diversion weir. The effect of weighting factors on the optimal outcomes is also investigated, and the implications for river management are discussed.

METHODS

In this section, the IFM used for regionalization of the natural flow regime is briefly summarized. The derived regional models for the 32 IHA are then scaled to the ungauged site using a distribution model. The IHA-based HMA used to assess flow regime alterations is described in the last part of this section.

Regionalization approach (RA)

The RA combines the available data from N sites in a homogeneous region to derive the regional model. The IFM is adopted herein because of its simplicity and popularity. The key assumption of the IFM is that the frequency distributions of the N sites are identical apart from a site-specific scaling factor, called 'index flood', that reflects the hydrologic and physiographic characteristics of a site. This relation can be expressed as

$$Q^{(i)}(F) = \mu^{(i)} Q^{(R)}(F), \quad i = 1, 2, \ldots, N \tag{1}$$

where $Q^{(i)}(F)$ is the quantile of nonexceedance probability F at site i, $\mu^{(i)}$ the index flood at site i, which is the mean value of the at-site frequency distribution, $Q^{(R)}(F)$ the regional quantile of nonexceedance probability F. It is assumed that the regional quantile function $Q^{(R)}(F)$ has a known form apart from p parameters $\theta_1^{(R)}, \cdots, \theta_p^{(R)}$, estimated with the at-site parameters weighted by the record length, that is

$$\theta_k^{(R)} = \frac{\sum_{i=1}^{N} n_i \theta_k^{(i)}}{\sum_{i=1}^{N} n_i}, \quad k = 1,2, \ldots, p \tag{2}$$

where n_i is the record length at site i, $\theta_k^{(i)}$ the kth parameter at site i, taken to be the L-moment and L-moment ratios of the non-dimensionalized data (=observed data scaled by the at-site index flood) (Hosking and Wallis, 1993). In other words, the parameters of the regional quantile function are the record-length weighted averages of the at-site L-moments and L-moment ratios.

L-moments are linear combinations of probability-weighted moments (Hosking, 1990), which can be expressed as

$$\lambda_{r+1} = \sum_{m=0}^{r} (-1)^{r-m} \binom{r}{m} \binom{r+m}{m} b_m \tag{3}$$

where λ_{r+1} is the $(r+1)$th L-moment, b_m the mth probability-weighted moment, defined as

$$b_m = \frac{1}{n} \sum_{j=r+1}^{n} \frac{(j-1)(j-2)\cdots(j-m)}{(n-1)(n-2)\cdots(n-m)} x_j \tag{4}$$

where x_j denotes the ordered data (i.e. $x_1 \leq x_2 \leq \ldots \leq x_n$), and n is the number of observed data. Hosking (1990) also defined L-moment ratios as

$$\tau = \frac{\lambda_2}{\lambda_1}, \quad \tau_r = \frac{\lambda_r}{\lambda_2}, \quad r = 3,4, \ldots \tag{5}$$

DOI: 10.1002/rra

where τ is the L-coefficient of variation or L-CV; τ_3 and τ_4 are the L-skewness and L-kurtosis factors, respectively. The at-site parameters $\theta_1^{(i)}$, $\theta_2^{(i)}$, $\theta_3^{(i)}$,..., $\theta_p^{(i)}$ are taken to be $\lambda_1^{(i)}$, $\tau^{(i)}$, $\tau_3^{(i)}$,..., $\tau_p^{(i)}$, respectively (Hosking and Wallis, 1993).

L-moment-based statistics for significance tests

Three L-moment-based statistics are used to detect the discordancy and heterogeneity of the data and select the candidate quantile functions (Hosking and Wallis, 1993). The first statistic is a discordancy measure, which is to identify those sites that are grossly discordant with the group as a whole. The discordancy measure for site i is given by

$$D_i = \frac{1}{3}(\mathbf{u}_i - \overline{\mathbf{u}})^T \mathbf{A}^{-1}(\mathbf{u}_i - \overline{\mathbf{u}}) \tag{6}$$

where $\mathbf{u}_i = \begin{bmatrix} \tau^{(i)} & \tau_3^{(i)} & \tau_4^{(i)} \end{bmatrix}^T$, $\overline{\mathbf{u}} = \left(\sum_{i=1}^{N} \mathbf{u}_i\right)/N$ is the group average vector, $\mathbf{A}$ the group covariance matrix, defined by $\mathbf{A} = \left[\sum_{i=1}^{N} (\mathbf{u}_i - \overline{\mathbf{u}})(\mathbf{u}_i - \overline{\mathbf{u}})^T\right]/(N-1)$. A larger value of D_i indicates a greater degree of discordancy. The criterion value of D_i used to decide whether a site is unusual depends on the total number of sites in a region, and can be found in Hosking and Wallis (1997).

The second statistic is a heterogeneity measure, which is to assess whether a group of sites may reasonably be treated as homogeneous. The heterogeneity measure is given by

$$H = \frac{V - \mu_V}{\sigma_V} \tag{7}$$

where V is the weighted standard deviation of the at-site L-CVs, μ_V and σ_V are the mean and standard deviation of the simulated V (for details see Hosking and Wallis, 1997). Hosking and Wallis (1993) suggested that a region is considered as homogeneous if $H < 1$, possibly heterogeneous if $1 \leq H < 2$, and definitely heterogeneous if $H \geq 2$.

The third statistic is a goodness-of-fit measure, which is to test whether a candidate distribution fits the data closely enough. The goodness-of-fit measure is given by

$$Z = \frac{\tau_4^{\text{Dist}} - \tau_4^{(R)} + B_4}{\sigma_4} \tag{8}$$

where $\tau_4^{\text{Dist}} = L$-kurtosis of candidate distribution, $\tau_4^{(R)} =$ regional L-kurtosis, B_4 and σ_4 are the simulation-based bias and standard deviation of $\tau_4^{(R)}$ (Hosking and Wallis, 1997). The criterion for accepting a candidate distribution is $|Z| \leq 1.64$ (Hosking and Wallis, 1993).

In this study, five commonly used distributions are taken to be the candidates for fitting the IHA at each site. They are all three-parameter distributions, including the generalized logistic (GLO), generalized extreme-value (GEV), three-parameter lognormal (LN3), Pearson type III (PE3) and generalized Pareto (GPA) distributions. Their cumulative distribution functions (cdf) are summarized in Appendix.

Distribution model for ungauged sites

The regional quantile functions $Q^{(R)}(F)$ derived for individual IHA can be scaled to the ungauged sites in the same region using the following distribution model:

$$Q^{(u)}(F) = f(A^{(u)})Q^{(R)}(F) \tag{9}$$

where $Q^{(u)}(F) =$ quantile function of the ungauged site; $f(A^{(u)}) =$ index flood $=$ mean value of each IHA, varying as a function of $A^{(u)}$, here $A^{(u)}$ is taken to be the drainage area at the ungauged site. Note that Equation (9) is analogous to Equation (1). The quantile functions so obtained represent the natural flow regime at the ungauged site, and the corresponding frequency histograms of individual IHA can be derived from these quantile functions. The HMA is then used to assess the flow regime alterations, as described in the following.

DOI: 10.1002/rra

Histogram matching approach (HMA)

The HMA is recently proposed by the authors (Shiau and Wu, 2008), which aims to eliminate the drawbacks of the RVA. The central idea behind the HMA is that two flow regimes would be similar if their corresponding frequency histograms of individual IHA exhibit resemblances, which can be measured using the 'statistical distances' between the natural and altered histograms. As such, flow regime alterations can be assessed with a distance-based dissimilarity metric. The procedure of HMA is briefly summarized here. The readers are referred to the original work for details.

The difference between two frequency histograms is indicated by a scaled 'degree of histogram dissimilarity', which is defined as

$$D_m = \frac{d_m}{\max(d_m)} \times 100\%, \quad m = 1, \ldots, 32 \tag{10}$$

where D_m = degree of histogram dissimilarity for the mth IHA, d_m = quadratic-form distance of the mth IHA, evaluated by

$$d_m = \sqrt{(|\mathbf{h} - \mathbf{k}|)^{\mathrm{T}} \mathbf{A} (|\mathbf{h} - \mathbf{k}|)}, \quad m = 1, \ldots, 32 \tag{11}$$

in which $\mathbf{h} = (h_1, h_2, \ldots, h_{n_c})^{\mathrm{T}}$ and $\mathbf{k} = (k_1, k_2, \ldots, k_{n_c})^{\mathrm{T}}$ are frequency vectors of the pre- and post-impact histograms H and K, respectively, where n_c = total number of classes; $|\mathbf{h} - \mathbf{k}|$ = statistical distance vector; $\mathbf{A} = [a_{ij}]$ = similarity matrix, where a_{ij} = similarity between class i of H and class j of K, and is given by

$$a_{ij} = \left(1 - \frac{d_{ij}}{d_{\max}}\right)^{\alpha} \tag{12}$$

where $d_{ij} = |V_i - V_j|$ = ground distance between class i of H and class j of K, in which V_i and V_j are mean values of classes i and j; $d_{\max} = \max(d_{ij}) = |V_1 - V_{n_c}|$; values of α range between 1 and ∞, here a linear similarity function with $\alpha = 1$ is adopted. An appropriate number of classes is determined by $n_c = rn^{1/3}/2r_{iq}$, where r = data range = difference between the 0.995- and 0.005-quantile values of a probability distribution; n = total number of data; r_{iq} = inter-quartile range = difference between the third- and first-quartile values. The maximum value of d_m is determined by $\max(d_m) = [4 - 2/(n_{c,m} - 1)]^{1/2}$, where $n_{c,m}$ = value of n_c adopted for the mth IHA.

Because individual values of D_m may exhibit different levels of dissimilarity, an integrative index is used to evaluate the 'overall degree of hydrologic alteration', that is

$$D_O = \left(\frac{1}{32}\sum_{m=1}^{32} D_m^2\right)^{\frac{1}{2}} \tag{13}$$

minimizing D_O is regarded as equivalent to best preserving the natural flow regime, thus is taken to be a surrogate objective of ecosystem needs in our case study, which is described in the following.

CASE STUDY

Overview of Kaoping Creek basin

The Kaoping Creek is located in Southern Taiwan (Figure 1), with a length of 171 km and a drainage area of 3257 km^2. The downstream alluvial plain is a major agricultural area. However, groundwater overdraft has caused negative impacts such as land subsidence and saltwater intrusion. To mitigate these impacts and provide an alternative source of water, currently two diversion facilities, that is, Kaoping and Chiahsien diversion weirs, are serving to supply stable water resources for domestic needs in the Kaoping Creek basin.

To further develop the water resources in the Kaoping Creek basin, several plans have been proposed. The Laonung diversion weir is among the proposed plans, and has passed the environmental impact assessment (WRA, 2003). The proposed Laonung diversion weir, located at the midstream Laonung Creek (a major tributary of the

DOI: 10.1002/rra

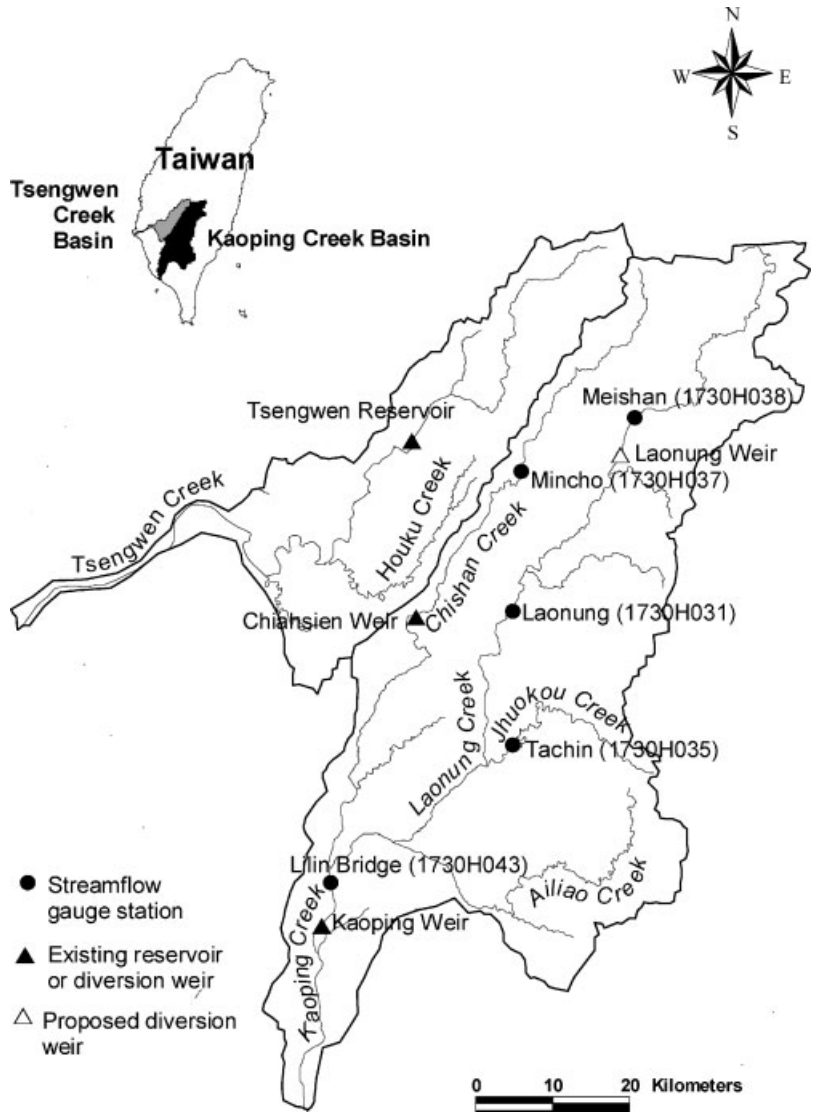

Figure 1. Location map of Kaoping Creek and Tsengwen Creek basins

Kaoping Creek), is an auxiliary facility for interbasin transfers of water to the Tsengwen reservoir (Figure 1). The design capacity of the proposed Laonung diversion weir is 50 m^3/s. The registered water rights for agricultural demands downstream of the Laonung diversion weir need to be reserved with higher priorities. The registered agricultural demands and projected interbasin transfers are shown in Table II, where the interbasin transfers are restricted in the high-flow months (May–October). The planning environmental flow scheme at the Laonung diversion weir is a release of 4.69 m^3/s, a low flow exceeded by 95% of daily flows (WRA, 2003).

Regionalization of natural flow regime

No flow records are available at the proposed Laonung weir site for evaluation of the natural flow regime, thus existing flow records in the Kaoping Creek basin are collected for construction of the regional models. After a careful review, five gauge stations are selected because of their record lengths and spatial distributions. The basic

DOI: 10.1002/rra

Table II. Registered agricultural demands and projected interbasin transfers at the proposed Laonung diversion weir (units in m^3/s)

Month	January	February	March	April	May	June	July	August	September	October	November	December
Registered agricultural demands	9.4	9.4	9.3	9.3	11.1	14.2	14.4	14.8	14.7	14.8	11.1	9.8
Projected interbasin transfers	0	0	0	0	50	50	50	50	50	50	0	0

information of these gauge stations is summarized in Table III, and their locations are shown in Figure 1. The record lengths of these gauge stations range from 11 to 48 years, the drainage areas of these stations range from 300 to 3000 km^2. The monthly mean flows at these stations are shown in Table IV, where highly fluctuating and unevenly distributed flow patterns are observed.

The regional models for individual IHA are constructed using the flow data available at these existing gauge stations. The procedure is as follows:

1. Computing the annual series of each IHA for all station sites.
2. Computing the mean value (i.e. scaling factor) of each IHA for all station sites.
3. Converting the annual series of each IHA to the non-dimensionalized annual series.
4. Computing *L*-moments and *L*-moment ratios of the non-dimensionalized annual series.
5. Combining the at-site parameters of each IHA into the regional parameters.
6. Computing the *L*-moment-based statistics.
7. Determining the best fit regional cdf model for each IHA.

The discordancy and heterogeneity measures (D_i and H) and the best-fit regional cdf models (with minimal $|Z|$) for all IHA are listed in Table V, which are summarized below.

Discordancy measures

The criterion value of D_i is 1.333 when the number of sites is equal to 5 (Hosking and Wallis, 1997). As shown in Table V, almost all the D_i values are less than this criterion. Only two sites (i.e. Laonung and Mincho stations) have

Table III. Basic information of five existing gauge stations in Kaoping Creek basin

Gauge station	Drainage area (km^2)	Record length (year)
Laonung (1730H031)	812.0	48 (1959–2006)
Tachin (1730H035)	360.2	19 (1964–1982)
Mincho (1730H037)	303.6	11 (1975–1985)
Meishan (1730H038)	391.7	17 (1977–1993)
Lilin Bridge (1730H043)	2894.8	14 (1991–2004)

Table IV. Monthly mean flows at existing gauge stations and proposed Laonung diversion weir site (units in m^3/s)

Station (or site)	January	February	March	April	May	June	July	August	September	October	November	December
Laonung	14.1	15.8	23.5	31.7	62.9	165.3	117.2	167.6	114.1	55.4	25.7	16.9
Tachin	5.3	4.5	4.9	6.3	29.3	121.6	84.7	108.3	58.5	31.6	10.5	6.2
Mincho	3.6	5.7	8.0	7.9	29.0	67.4	49.0	67.9	37.6	13.9	6.4	4.2
Meishan	7.5	10.6	15.4	21.9	33.8	67.8	40.5	57.5	48.4	22.6	13.2	8.7
Lilin Bridge	31.2	40.3	52.1	63.5	157.3	431.9	461.8	659.5	406.8	158.4	76.3	43.3
Laonung weir	10.4	13.0	18.7	22.4	53.6	146.5	122.6	172.0	108.1	46.9	21.8	13.2

DOI: 10.1002/rra

Table V. Discordancy and heterogeneity measures D_i and H, best fit regional cdf models with minimal $|Z|$, relations between scaling factor μ and drainage area A and the corresponding coefficients of determination R^2 (for 32 IHA)

IHA	D_i	H	$\|Z\|$	Best fit regional cdf model	Scaling factor	R^2
January	<1.333	−0.302	0.140	GLO ($\xi=0.919$, $\alpha=0.151$, $k=-0.295$)	$\mu=-65.6+27.8\log(A)$	0.99
Febuary	<1.333	1.959	0.048	GEV ($\xi=0.680$, $\alpha=0.251$, $k=-0.419$)	$\mu=-84.3+35.6\log(A)$	0.97
March	<1.333	0.629	0.821	GLO ($\xi=0.651$, $\alpha=0.223$, $k=-0.588$)	$\mu=-108.2+46.1\log(A)$	0.97
April	<1.333	−0.056	0.004	GEV ($\xi=0.511$, α=0.333, $k=-0.480$)	$\mu=-131.8+56.4\log(A)$	0.96
May	<1.333	−0.600	0.173	GEV ($\xi=0.646$, $\alpha=0.466$, $k=-0.157$)	$\mu=-312.8+134.0\log(A)$	0.97
June	<1.333	−0.242	0.192	GEV ($\xi=0.675$, $\alpha=0.479$, $k=-0.093$)	$\mu=-851.7+365.1\log(A)$	0.95
July	<1.333	−0.779	0.099	GLO ($\xi=0.814$, $\alpha=0.603$, $k=-0.569$)	$\mu=-1022.1+418.7\log(A)$	0.92
August	<1.333	−0.451	1.475	GPA ($\xi=0.152$, $\alpha=1.032$, $k=0.218$)	$\mu=-1479.1+603.9\log(A)$	0.92
September	<1.333	−0.569	0.002	GLO ($\xi=0.808$, $\alpha=0.283$, $k=-0.355$)	$\mu=-918.2+375.4\log(A)$	0.95
October	<1.333	−0.623	0.125	GLO ($\xi=0.837$, $\alpha=0.483$, $k=-0.614$)	$\mu=-346.5+143.9\log(A)$	0.97
November	<1.333	1.619	1.622	GLO ($\xi=0.877$, $\alpha=0.198$, $k=-0.331$)	$\mu=-170.7+70.4\log(A)$	0.97
December	<1.333	1.616	4.278	GLO ($\xi=0.921$, $\alpha=0.168$, $k=-0.262$)	$\mu=-94.8+39.5\log(A)$	0.99
1-day min	<1.333	1.073	0.785	GLO ($\xi=1.013$, $\alpha=0.190$, $k=0.041$)	$\mu=-30.3+13.2\log(A)$	0.99
3-day min	<1.333	0.540	1.365	GLO ($\xi=1.008$, $\alpha=0.180$, $k=0.026$)	$\mu=-32.2+14.0\log(A)$	0.99
7-day min	<1.333	0.198	1.850	GLO ($\xi=1.001$, $\alpha=0.173$, $k=0.004$)	$\mu=-33.6+14.6\log(A)$	0.99
30-day min	<1.333	−0.577	1.525	GLO ($\xi=0.958$, $\alpha=0.158$, $k=-0.156$)	$\mu=-43.9+18.8\log(A)$	0.99
90-day min	<1.333	0.746	0.134	GLO ($\xi=0.859$, $\alpha=0.193$, $k=-0.375$)	$\mu=-79.8+33.4\log(A)$	0.98
1-day max	<1.333	1.623	0.263	PE3 ($\eta=1.000$, $\sigma=0.577$, $\gamma=0.497$)	$\mu=-10523.1+4355.8\log(A)$	0.92
3-day max	<1.333	1.049	0.498	PE3 ($\eta=1.000$, $\sigma=0.550$, $\gamma=0.926$)	$\mu=-7565.2+3122.0\log(A)$	0.92
7-day max	<1.333	0.790	0.179	PE3 ($\eta=1.000$, $\sigma=0.509$, $\gamma=0.828$)	$\mu=-5360.9+2196.3\log(A)$	0.92
30-day max	<1.333	0.675	0.660	GEV ($\xi=0.824$, $\alpha=0.378$, $k=0.127$)	$\mu=-2331.9+956.3\log(A)$	0.93
90-day max	<1.333	−0.607	0.742	GEV ($\xi=0.963$, $\alpha=0.232$, $k=-0.095$)	$\mu=-1279.6+529.1\log(A)$	0.93
Base flow	<1.333	0.026	1.895	GLO ($\xi=0.924$, $\alpha=0.241$, $k=-0.192$)	$\mu=0.124$	
1-day min date	>1.333	−0.089	0.201	GLO ($\xi=0.972$, $\alpha=0.362$, $k=-0.153$)	$\mu=132.3$	
1-day max date	<1.333	−1.276	1.525	GEV ($\xi=0.940$, $\alpha=0.182$, $k=0.313$)	$\mu=207.4$	
Low count	<1.333	0.334	0.323	GLO ($\xi=0.909$, $\alpha=0.304$, $k=-0.178$)	$\mu=2.2+0.8\log(A)$	0.89
Low duration	<1.333	−0.288	0.265	GEV ($\xi=0.842$, $\alpha=0.299$, $k=0.062$)	$\mu=92.0$	
High count	<1.333	−0.376	1.062	PE3 ($\eta=1.000$, $\sigma=0.411$, $\gamma=0.656$)	$\mu=1.3+1.7\log(A)$	0.88
High duration	<1.333	−1.654	0.472	GLO ($\xi=1.028$, $\alpha=0.206$, $k=0.081$)	$\mu=91.5$	
Fall rate	<1.333	−0.779	0.488	PE3 ($\eta=1.000$, $\sigma=0.534$, γ=1.147)	$\mu=142.4-58.6\log(A)$	0.91
Rise rate	<1.333	−0.541	0.073	GLO ($\xi=0.864$, $\alpha=0.537$, $k=-0.477$)	$\mu=-377.1+159.2\log(A)$	0.92
Flow reversal	<1.333	0.329	0.361	PE3 ($\eta=1.000$, $\sigma=0.342$, $\gamma=1.272$)	$\mu=3.6+16.9\log(A)$	0.77

their D_i values (=1.438 and 1.468) for a single IHA (i.e. date of 1-day minimum flow) slightly greater than 1.333 but less than the criterion value of D_i for six sites (=1.648). Thus, the two sites are not considered as significantly discordant with other sites.

Heterogeneity measures

The homogeneous criterion ($H<1$) is met by most of the IHA, except that six IHA, that is, monthly flows of February, November and December, annual 1-day minimum flow, and annual 1- and 3-day maximum flows, indicate a possibly heterogeneous region ($1\le H<2$). Thus, it is assumed that the Kaoping Creek basin is a reasonably homogeneous region.

Goodness-of-fit measures

The $|Z|$ values associated with the best fit regional cdf models are mostly smaller than the criterion (= 1.64) for accepting a candidate distribution. Only three IHA, that is, monthly flow of December, annual 7-day minimum flow, and base flow condition, have all their $|Z|$ values associated with five candidate distributions greater than the criterion. For simplicity, the candidate distributions with the smallest $|Z|$ values are adopted here as the regional cdf models for these three IHA.

DOI: 10.1002/rra

To further test the reliability of the derived regional models (i.e. the best fit cdf models and scaling factors), the histograms of 32 IHA at the five existing stations are constructed using these regional models. Differences between the constructed and observed histograms are measured by the mean value of 32 degrees of histogram dissimilarity. The mean degrees of histogram dissimilarity at these existing stations range from 14.8% to 25.4%, indicating that the errors associated with the derived regional models are within an acceptable range.

Here, we take the mean flow of January as an example to illustrate how the cdf at an ungauged site is obtained using the derived regional model. The best fit regional cdf model for the mean flow of January is GLO distribution (see Table V). Based on the IFM, the cdf at site i can be expressed as

$$F(x) = \frac{1}{1 + \left[1 + 1.95\left(\frac{x}{\mu^{(i)}} - 0.919\right)\right]^{-3.39}} \tag{14}$$

where $\mu^{(i)}$ = scaling factor (or index flood) at site i, which is taken to be the mean value of each IHA. The best-fit cdfs for the five existing stations are shown in Figure 2(a) (with their scaling factors being 14.1, 5.3, 3.6, 7.5 and 31.2 m^3/s, respectively), where the observed data demonstrate satisfactory agreement with the best fit cdfs. Shown in Figure 2(b) are the observed data and best fit cdfs of five IHA selected from different groups, which include the mean flow of April (G1), annual 30-day maximum flow (G2), date of annual 1-day minimum flow (G3), high pulse

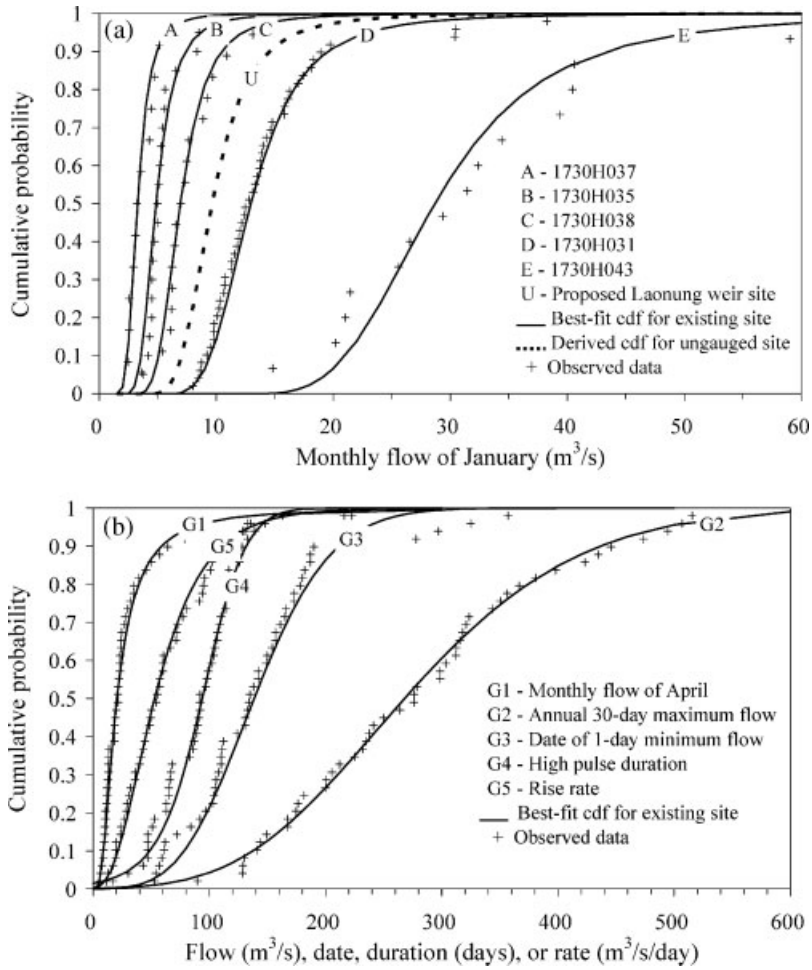

Figure 2. (a) Best fit and derived cdfs and observed data for monthly flow of January at five existing gauge stations and proposed Laonung diversion weir site; (b) best fit cdfs and observed data for five IHA at Laonung gauge station

DOI: 10.1002/rra

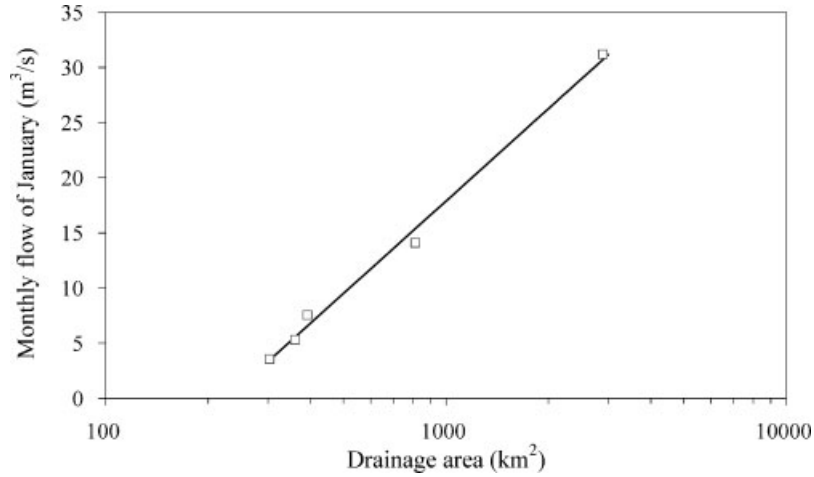

Figure 3. Relation between monthly flow of January and drainage area at five existing gauge stations ($R^2 = 0.99$)

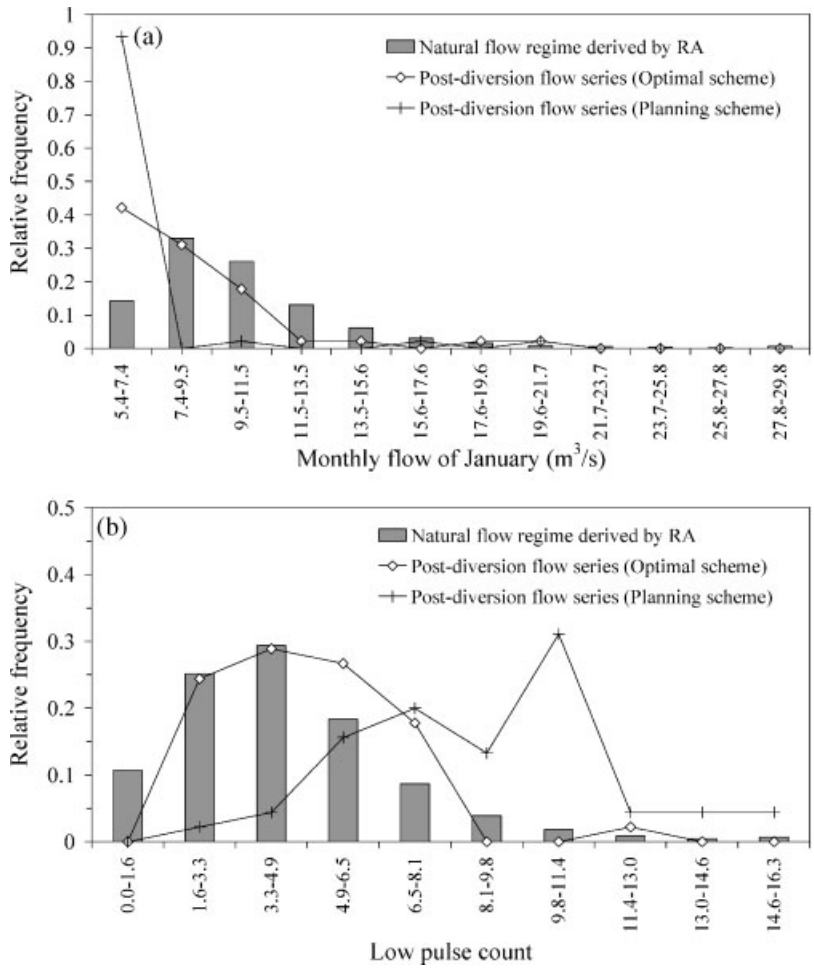

Figure 4. Comparisons between the frequency histograms of RA-based natural flow regime and post-diversion flow series (optimal and planning environmental flow schemes) at proposed Laonung diversion weir site for (a) monthly flow of January and (b) low pulse count

DOI: 10.1002/rra

duration (G4) and flow rise rate (G5) at the Laonung gauge station. The observed data of these IHA also exhibit satisfactory agreement with their best fit cdfs.

Natural flow regime at ungauged site

To apply Equation (9), the relations between scaling factor and drainage area at the ungauged site are established for individual IHA, which are summarized in Table V together with the corresponding coefficients of determination R^2. The scaling factors of some IHA (i.e. base flow, dates of annual 1-day maximum and minimum flows, low and high pulse durations) exhibit no significant correlations to the drainage area and are probably related to other characteristics of the drainage basin, thus are taken to be constant for simplicity. As an illustration example, the relation between the mean flow of January and drainage area, derived with the data from five existing stations, is given below (shown in Figure 3):

$$\mu^{(i)} = -65.6 + 27.8 \times \log(A^{(i)}), \quad R^2 = 0.99 \tag{15}$$

in which $\mu^{(i)}$ = mean flow of January (m^3/s) at site i, and $A^{(i)}$ = drainage area (km^2) at site i. As such, the value of $\mu^{(i)}$ at an ungauged site can be determined with the given value of $A^{(i)}$ and the cdf at this ungauged site is obtained by Equation (14). It should be noted that the derived relations between the scaling factor and drainage area are not recommended for use beyond their applicable range of drainage area (between 300 and 3000 km^2). Given the drainage area of 542 km^2 at the proposed Laonung diversion weir site, the monthly mean flows can be evaluated (Table IV), and the cdf for the mean flow of January is obtained and shown in Figure 2(a). The frequency histograms derived from this cdf are shown in Figure 4(a), which are then compared to the histograms of the post-diversion flows for assessment of the flow regime alterations. The post-diversion flow series are obtained via the weir operation model, as described below.

Weir operation model

The water-supply objectives of the proposed Laonung diversion weir are to meet the agricultural and interbasin transfer water demands. Since the post-diversion flows vary as a function of environmental flow prescriptions, a weir operation model is used to simulate the flows diverted for water supplies and released for ecosystem preservation.

The system of flows at the proposed Laonung diversion weir site is depicted in Figure 5, where three criteria are considered at time t, including the environmental flow prescription Q^t_{EF}, registered agricultural demand Q^t_{A} and projected interbasin transfer Q^t_D; Q^t_{I} denotes the natural (or pre-diversion) inflow; Q^t_{AA} denotes the amount of flow actually diverted for supplying agricultural demands; Q^t_{AD} denotes the amount of flow actually diverted for interbasin transfer; Q^t_{O} denotes the post-diversion outflow. The registered agricultural demands Q^t_{A} and projected interbasin transfers Q^t_D are given in Table II, as such Q^t_{EF} are the only decision variables to be specified. In this study, a monthly varying environmental flow scheme is adopted, thus a total of 12 Q^t_{EF} values are prescribed. The priorities of water allocation are: the first priority is given to the environmental flows, the second is given to the registered agricultural demands and the lowest priority is given to the projected interbasin transfers. The operating rules of the proposed Laonung diversion weir are given as follows:

$$\begin{cases} Q^t_{\mathrm{O}} = Q^t_{\mathrm{I}}, Q^t_{\mathrm{AA}} = 0, Q^t_{\mathrm{AD}} = 0 & \text{if } Q^t_{\mathrm{I}} < Q^t_{\mathrm{EF}} \\ Q^t_{\mathrm{O}} = Q^t_{\mathrm{EF}}, Q^t_{\mathrm{AA}} = Q^t_{\mathrm{I}} - Q^t_{\mathrm{EF}}, Q^t_{\mathrm{AD}} = 0 & \text{if } Q^t_{\mathrm{EF}} \le Q^t_{\mathrm{I}} < Q^t_{\mathrm{EF}} + Q^t_{\mathrm{A}} \\ Q^t_{\mathrm{O}} = Q^t_{\mathrm{EF}}, Q^t_{\mathrm{AA}} = Q^t_{\mathrm{A}}, Q^t_{\mathrm{AD}} = Q^t_{\mathrm{I}} - Q^t_{\mathrm{EF}} - Q^t_{\mathrm{A}} & \text{if } Q^t_{\mathrm{EF}} + Q^t_{\mathrm{A}} \le Q^t_{\mathrm{I}} < Q^t_{\mathrm{EF}} + Q^t_{\mathrm{A}} + Q^t_{\mathrm{D}} \\ Q^t_{\mathrm{O}} = Q^t_{\mathrm{I}} - Q^t_{\mathrm{AA}} - Q^t_{\mathrm{AD}}, Q^t_{\mathrm{AA}} = Q^t_{\mathrm{A}}, Q^t_{\mathrm{AD}} = Q^t_{\mathrm{D}} & \text{if } Q^t_{\mathrm{I}} > Q^t_{\mathrm{EF}} + Q^t_{\mathrm{A}} + Q^t_{\mathrm{D}} \end{cases} \tag{16}$$

The post-diversion flows, Q^t_{O}, are used to assess the degree of hydrologic alteration. The flow series actually diverted for supplying the agricultural demands and interbasin transfers, Q^t_{AA} and Q^t_{AD}, are used to evaluate the water-supply performances, which are indicated by the shortage ratio and annual interbasin transfers, as described in the following.

DOI: 10.1002/rra

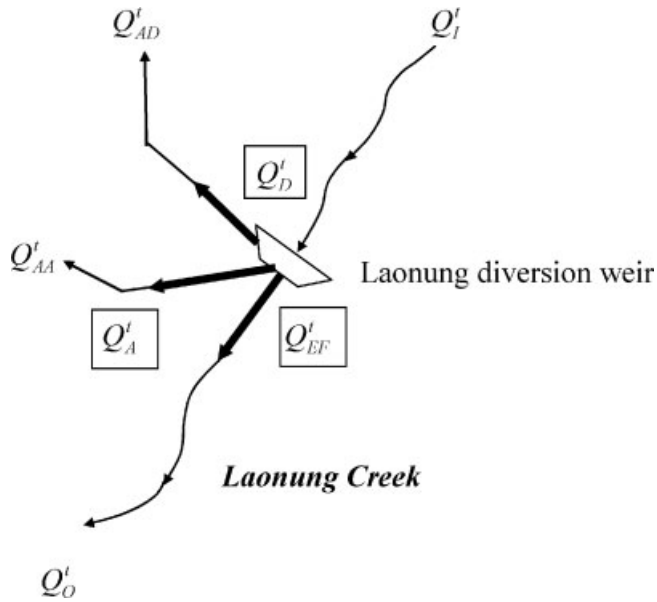

Figure 5. System of flows at proposed Laonung diversion weir site. Flows in the boxes are environmental flow prescriptions Q^t_{EF}, registered agricultural demands Q^t_{A} and projected interbasin transfers Q^t_D; Q^t_{I} and Q^t_{O} denote inflows and outflows; Q^t_{AA} and Q^t_{AD} denote the flows actually diverted for agricultural demands and interbasin transfers, respectively; superscripts t denote time

Indices of water-supply performances

The water-supply deficit for the agricultural demands is expressed by a shortage ratio, defined as the ratio of total water deficit to total demand over a time period. The shortage ratio for the registered agricultural water demands, denoted as SR, is evaluated with

$$\mathrm{SR} = \frac{\sum_{t=1}^{\mathrm{ND}} \left|\min\left\{Q^t_{\mathrm{AA}} - Q^t_{\mathrm{A}}, 0\right\}\right|}{\sum_{t=1}^{\mathrm{ND}} Q^t_{\mathrm{A}}} \times 100\% \tag{17}$$

where ND = total number of days within the study period.

The performance of interbasin transfers is indicated by the annual diversion, defined as the average amount of water diverted for interbasin transfers in a year. The annual diversion for the interbasin transfers, denoted as AD, is evaluated with

$$\mathrm{AD} = \frac{\sum_{t=1}^{\mathrm{ND}} Q^t_{\mathrm{AD}}}{(\mathrm{ND}/365)} \tag{18}$$

Both SR and AD are the human needs objectives to be optimized with the aggregated multiobjective optimization algorithm, which is described as follows.

Aggregated multiobjective optimization

The operational goal of the proposed Laonung diversion weir is to supply water for human demands while sustaining the downstream natural flow regime, which formulates a typical multiobjective optimization problem.

DOI: 10.1002/rra

The objective function can be expressed as

$$\text{Min}\,\{D_{\text{O}}\},\ \text{Min}\,\{\text{SR}\}\ \text{and}\ \text{Max}\,\{\text{AD}\} \tag{19}$$

Optimization problems involving multiple conflicting objectives introduce Pareto tradeoff solutions rather than a single optimal solution. Because the aim of this study is to derive the regional natural flow regime and seek an optimal environmental flow scheme at an ungauged site rather than fully explore the Pareto tradeoff solutions, an aggregated multiobjective optimization genetic algorithm is used instead to find the optimal solution of a rescaled and aggregated objective function, which is expressed by

$$\text{Min}\,L = \text{Min}\left[\left(w_1\frac{D_{\text{O}}-D_{\text{O,min}}}{D_{\text{O,max}}-D_{\text{O,min}}}\right)^2+\left(w_2\frac{\text{SR}-\text{SR}_{\text{min}}}{\text{SR}_{\text{max}}-\text{SR}_{\text{min}}}\right)^2+\left(w_3\frac{\text{AD}_{\text{max}}-\text{AD}}{\text{AD}_{\text{max}}-\text{AD}_{\text{min}}}\right)^2\right]^{\frac{1}{2}} \tag{20}$$

where L is the value of objective function; the subscripts max and min denote the maximum and minimum values; w_1, w_2 and w_3 are the weighting factors, by definition $w_1+w_2+w_3=1$. The values of $D_{\text{O,max}}$, SR_{min} and AD_{max} are obtained with an extreme condition of $Q^t_{\text{EF}}=0$, whereas $D_{\text{O,min}}$, SR_{max} and AD_{min} correspond to $Q^t_{\text{AD}}=0$ and $Q^t_{\text{AA}}=0$. The optimal set of Q^t_{EF} is sought with a simple genetic algorithm (Haupt and Haupt, 2004), the population size = 1000, crossover and mutation rates = 0.8 and 0.05, respectively. The selection, crossover and mutation operators are used to iteratively evolve a population towards the true optimal solution. The procedure is repeated until a stable solution is reached. The optimal solution so obtained is a compromise between the human and ecosystem needs objectives.

RESULTS AND DISCUSSION

Optimal environmental flows

To determine the optimal environmental flows by the weir operation model, the input data of inflow series Q^t_{I} are needed. A synthetic daily flow series (1959–2003) based on the area ratio method (WRA, 2003) is employed in this study. This flow series has been used by the Water Resources Agency (Taiwan) for evaluation of the proposed Laonung diversion weir. Equal weights, $w_1=w_2=w_3=1/3$, are assigned to the three objectives in Equation (20). The limiting values used here are $D_{\text{O,max}}=60.8\%$, $\text{SR}_{\text{min}}=2.9\%$ and $\text{AD}_{\text{max}}=370\times10^6\,\text{m}^3$; $D_{\text{O,min}}=27.9\%$, $\text{SR}_{\text{max}}=32.1\%$ and $\text{AD}_{\text{min}}=0\,\text{m}^3$. It should be noted here that the value of $D_{\text{O,min}}$ is apart from 0 because the histogram derived from the RA-based natural flow regime is slightly different from that derived from the synthetic input flow series.

The resulting optimal outcomes are $D_{\text{O}}=39.6\%$, $\text{SR}=14.1\%$ and $\text{AD}=299.4\times10^6\,\text{m}^3$, with the corresponding optimal environmental flow prescriptions listed in Table VI. These environmental flows range from 6.5 to 37 m^3/s, prescribed for April and March, respectively. The environmental flows in the wet period (May–October) are almost identically 8.5 m^3/s, while those in the dry months (November–January) all exceed 10 m^3/s. Such a result is consistent with those of previous work (Shiau and Wu, 2006, 2007a). As a comparison, the outcomes associated with the planning scheme of constant environmental flow (=4.69 m^3/s) are $D_{\text{O}}=54.9\%$, $\text{SR}=8.3\%$ and $\text{AD}=328.4\times10^6\,\text{m}^3$. The optimal scheme significantly improves the ecosystem needs objective by a 15.3% reduction in D_{O}, which is achieved at the cost of slightly increasing SR by 5.8% and decreasing AD by $29\times10^6\,\text{m}^3$ ($\sim$9% reduction).

The values of D_m for the 32 IHA associated with the optimal and planning schemes are summarized in Table VII. It is shown that the values of D_m associated with the planning constant scheme are consistently higher than those

Table VI. The optimal environmental flow prescriptions at the proposed Laonung diversion weir (units in m^3/s)

Month	January	February	March	April	May	June	July	August	September	October	November	December
Q^t_{EF}	11.2	7.4	37.0	6.5	8.5	8.5	8.5	8.8	8.5	8.5	14.9	15.2

DOI: 10.1002/rra

Table VII. Degrees of histogram dissimilarity (for 32 IHA) associated with the optimal and planning environmental flow schemes at the proposed Laonung diversion weir

	IHA	Degree of histogram dissimilarity (%)	
		Optimal scheme	Planning scheme
Group 1	January	27.1	76.3
	Febuary	41.2	47.4
	March	18.9	30.3
	April	33.9	36.3
	May	54.4	60.9
	June	47.6	47.6
	July	50.3	52.5
	August	36.9	36.9
	September	57.0	59.2
	October	56.6	58.8
	November	33.7	65.2
	December	20.6	78.9
Group 2	1-day min	22.7	59.2
	3-day min	28.6	65.0
	7-day min	34.2	59.9
	30-day min	29.1	73.8
	90-day min	33.8	68.7
	1-day max	39.3	39.3
	3-day max	35.9	35.9
	7-day max	48.1	48.1
	30-day max	56.4	56.4
	90-day max	74.4	74.4
	Base flow	40.1	41.4
Group 3	Julian date of 1-day min	17.2	44.4
	Julian date of 1-day max	17.9	17.9
Group 4	Low pulse count	16.5	52.4
	High pulse count	14.1	16.4
	Low pulse duration	31.3	80.1
	High pulse duration	64.8	66.8
Group 5	Fall rate	2.6	23.6
	Rise rate	4.5	23.0
	Number of flow reversal	53.1	66.0

associated with the optimal scheme, which is especially true for the low-flow IHA. Two such examples, that is, the monthly flow of January (Group 1) and low pulse count (Group 4), are demonstrated in Figure 4, where the frequency histograms of the natural and post-diversion flow series are compared. The results reveal that the frequency histogram associated with the optimal scheme exhibits better resemblance to that of the natural flow regime, while the frequency histogram associated with the planning constant scheme is less similar to the natural one. The values of D_m for the monthly flow of January associated with the optimal and planning schemes are 27.1 and 76.3%, respectively. To further demonstrate the difference between the two post-diversion flow regimes, the time series plots for the monthly flow of January are shown in Figure 6, where the post-diversion flow series associated with the optimal scheme exhibits much closer resemblance to the natural flow series. Similarly, for the low pulse count the value of D_m associated with the optimal scheme ($= 16.5\%$) is much smaller than that associated with the planning scheme ($= 52.4\%$). Both of these results indicate that the natural flow regime is better preserved with the optimal time-varying environmental flow scheme.

A comment on the RA-based natural flow regime is given as follows. The natural flow regime derived for an ungauged site is used for assessment of hydrologic alterations, which then provide a basis for seeking the optimal environmental flows. Although the optimal value of D_O ($= 39.6\%$) may seem a little too high, thus casting

DOI: 10.1002/rra

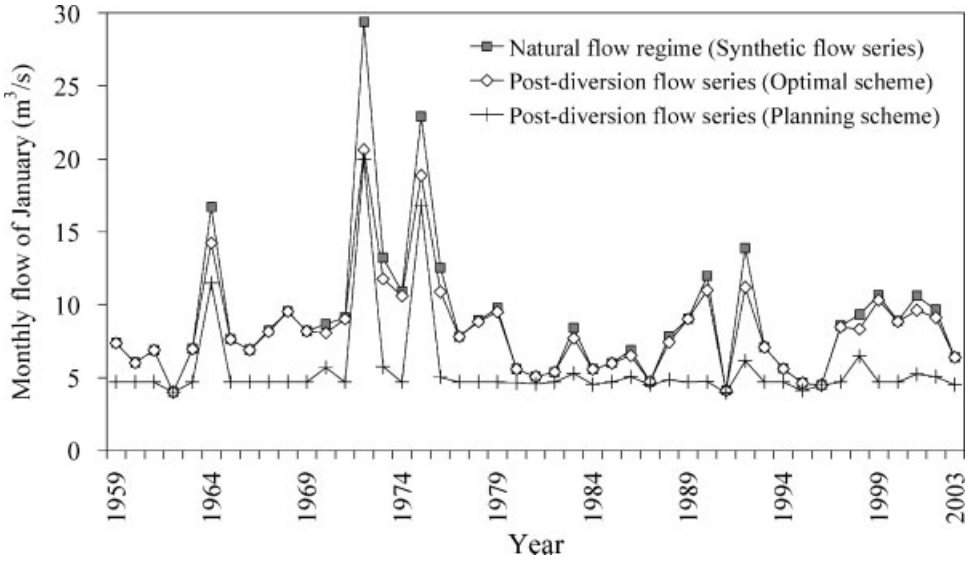

Figure 6. Time series plots of natural and post-diversion monthly flows of January at proposed Laonung diversion weir site

skepticism on the RA-based natural flow regime, such an outcome is in fact attributed to the discrepancy between the RA-based natural flow regime and synthetic pre-diversion flow series at the ungauged site, as evidenced by the non-zero value of $D_{O,min}$. Despite this inherent discrepancy existing between the different approaches to generating flow data at ungauged sites, the optimal outcomes resulting from the RA-based natural flow regime, including the optimal values of Q_{EF}^{t} and D_m, appear to be plausible and consistent with those reported in the previous work, thus validating the RA employed in this study.

Effect of weighting factors

In this section, we explore the effect of weighting factors on the outcomes associated with the optimal environmental flow scheme. The contour plots of the optimal D_O, SR, AD and L for various combinations of weighting factors are illustrated in Figure 7, where only two factors are shown in each plot because the third one can be obtained by the relation $w_1 + w_2 + w_3 = 1$. Figure 7 consistently reveals that w_1 is the weighting factor that dominates the optimal outcomes. For example, Figure 7(a) reveals that the optimal value of D_O decreases significantly as w_1 is shifted from the dashed diagonal ($w_1 = 0$) towards the lower-left corner ($w_1 = 1$), indicating that the hydrologic alteration is reduced as more weight is given to the ecosystem needs objective. Figure 7(b) and (c) reveal that w_1 not only dominates the optimal value of D_O, but also affects the optimal outcomes of SR and AD; the values of w_2 and w_3, however, have minor effects on these optimal outcomes. As such, two extreme outcomes are associated with two extreme values of w_1. The first corresponds to $w_1 = 1$, which leads to the outcomes of $D_{O,min} = 27.9\%$ (Figure 7(a)), $SR_{max} = 32.1\%$ (Figure 7(b)) and $AD_{min} = 0\,m^3$ (Figure 7(c)). The second corresponds to $w_1 = 0$, leading to the outcomes of $D_{O,max} = 60.8\%$ (Figure 7(a)), $SR_{min} = 2.9\%$ (Figure 7(b)) and $AD_{max} = 370 \times 10^6\,m^3$ (Figure 7(c)). Figure 7(d) reveals that the minimum L also occurs at these two extreme values of w_1, implying that the global optimal solution is obtained as a full or null weighting is assigned to the ecosystem needs objective. On the other hand, the maximum L is obtained with $w_1 = 0.4$, $w_2 = 0.6$ and $w_3 = 0$, which leads to the outcomes of $D_O = 42.2\%$, $SR = 12.9\%$ and $AD = 299.8 \times 10^6\,m^3$, indicating that the least optimal solution is obtained as the interbasin transfer objective is given a null weighting while the agricultural demands objective is given more weight than the ecosystem needs objective. The dominance of w_1 on the optimal outcomes is attributed to the fact that the ecosystem needs objective is given the highest priority in the weir operation model. Lower priorities for the human needs objectives and restrictions on water diversions, on the other hand, result in the less dominance of w_2 and w_3 on the optical outcomes.

DOI: 10.1002/rra

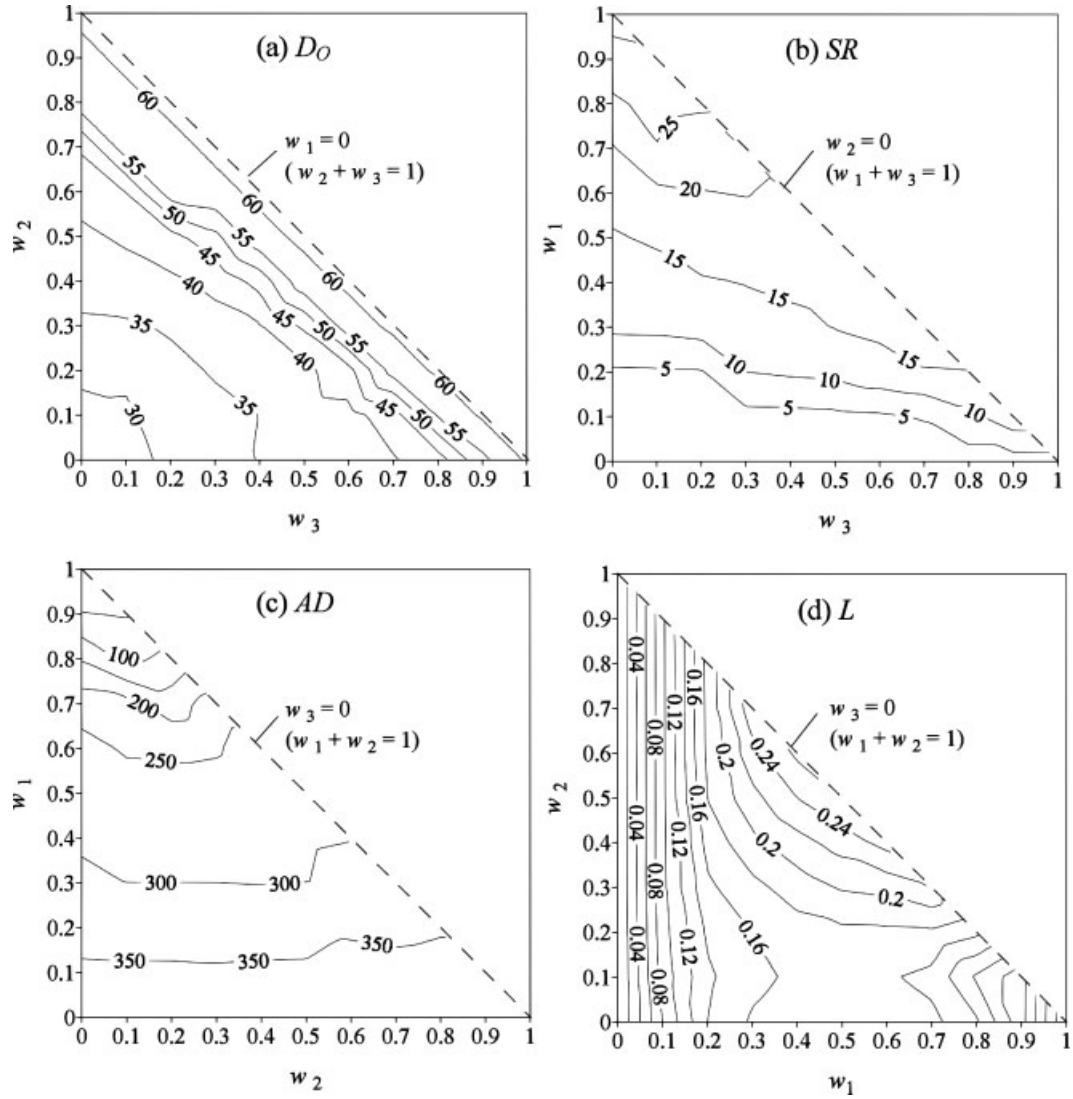

Figure 7. Contour plots of optimal outcomes: (a) D_O, (b) SR, (c) AD ($10^6\,m^3$) and (d) L for various combinations of weighting factors

To further demonstrate the dominance of w_1, the envelope curves of the optimal D_O, SR and AD varying with w_1 are shown in Figure 8(a), where the maximum bandwidths of the envelope curves corresponding to different values of w_2 and w_3 are much smaller than their maximum ranges of variation corresponding to two extreme values $w_1 = 0$ and 1, indicating that w_1 has major influences on the optimal outcomes. The envelope curves of the optimal outcomes varying with w_2 are shown in Figure 8(b), where the maximum bandwidths of the envelope curves are much greater, the bandwidths reduce with increasing w_2 and the three sets of envelope curves converge to an extreme outcome at $w_2 = 1$. The three horizontal curves, however, correspond to the extreme outcome with $w_1 = 0$. Variations of the optimal AD with w_2 for some specific values of w_3 are demonstrated in Figure 8(c), where two distinct trends of variation are observed. First, for a specific value of w_3, the value of *AD* increases with w_2 because of the reduction in w_1. Second, the maximum range of variation in AD reduces with increasing w_3 because of the reduced range of variation in w_1; the upper bounds of these AD curves correspond to the extreme outcome with $w_1 = 0$. Both of these trends reconfirm the major influences of w_1 on the optimal outcomes.

River managers and decision makers may select an operation strategy for the proposed Laonung diversion weir based on the results demonstrated in Figures 7 and 8. For example, if the ecosystem needs objective of the proposed

DOI: 10.1002/rra

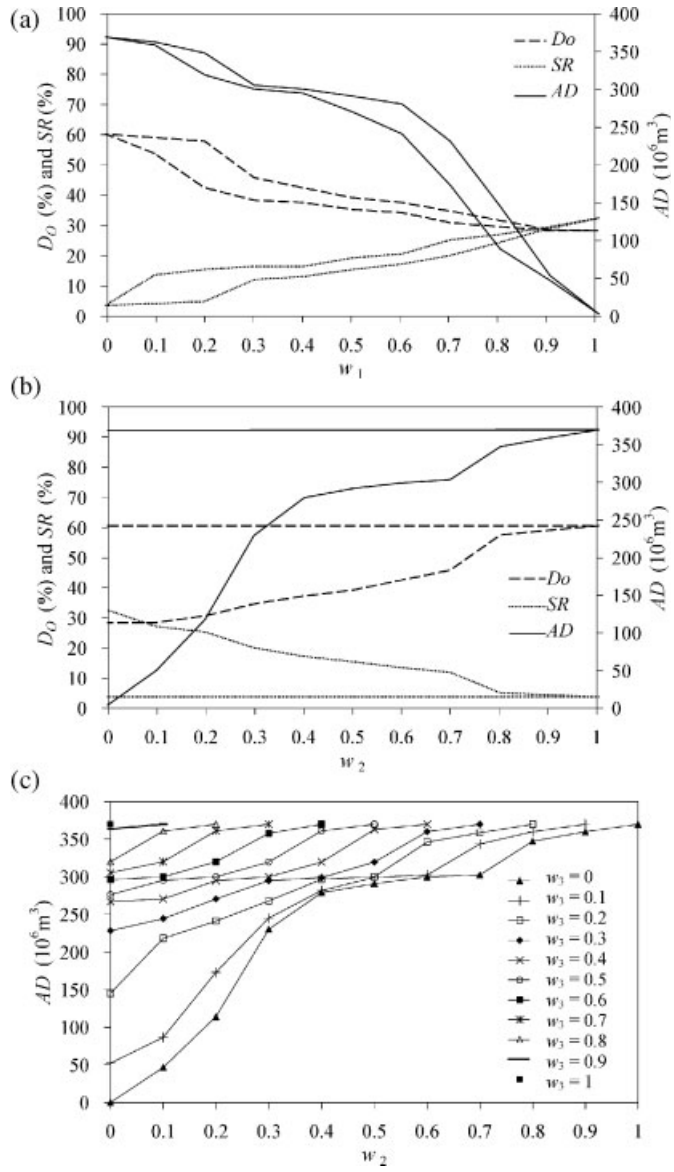

Figure 8. (a) Envelope curves of optimal outcomes varying with w_1; (b) envelope curves of optimal outcomes varying with w_2; (c) variations of optimal *AD* with w_2 for some specific values of w_3

Laonung diversion weir is to maintain a value of $D_O < 35\%$, then a value of $w_1 > 0.7$ is recommended (Figure 7(a)), which will lead to the outcomes of SR ranging between 19.6 and 32.1% and AD $< 230 \times 10^6$ m^3 (Figure 8(a)). If, on the other hand, the annual interbasin transfer AD is expected to exceed 300×10^6 m^3 due to the drought events, then a value of $w_1 < 0.3$ should be used (Figure 7(c)), which will however result in the ranges of D_O between 39.7 and 60.8% and SR between 2.9 and 15.9% (Figure 8(a)).

CONCLUSIONS

In this work we employed the RA to derive the natural flow regime at an ungauged site. The RA-based natural flow regime, expressed by the histograms of 32 IHA, was integrated with the HMA to seek the optimal environmental

DOI: 10.1002/rra

flow scheme for the proposed Laonung diversion weir. The results reveal that the environmental flow prescriptions in the wet period are consistently smaller than those specified in the dry period. The outcomes associated with the planning constant scheme are significantly improved by the optimal time-varying scheme, including a 15.3% reduction in the ecosystem need objective, achieved at the cost of a 5.8% increase in the shortage ratio of agricultural demands and a 9% reduction in the annual interbasin transfers. The histogram dissimilarities of 32 IHA associated with the planning constant scheme are consistently greater than those associated with the optimal scheme, especially for the low-flow IHA, indicating that the natural flow regime is better preserved with the optimal scheme presented herein. Despite the inherent discrepancy existing between the different approaches to generating flow data at the ungauged site, the optimal outcomes resulting from the RA-based natural flow regime appear to be plausible and consistent with those reported in the previous work, thus validating the RA employed in this study.

We also explored the effect of weighting factors on the outcomes associated with the optimal scheme. The results reveal that the weighting factor of the ecosystem need objective, w_1, dominates all optimal outcomes, while the weighting factors of the agricultural demand and interbasin transfer objectives, w_2 and w_3, have minor effects on the optimal outcomes. Two extreme outcomes are associated with two extreme values of w_1, that is, $w_1 = 1$ leads to the outcomes of $D_{O,min}$, SR_{max} and AD_{min}, while $w_1 = 0$ leads to the outcomes of $D_{O,max}$, SR_{min} and AD_{max}. The minimum L also occurs at these two extreme values of w_1, implying that the global optimal solution is obtained with a full or null weighting assigned to the ecosystem need objective. On the other hand, the least optimal solution is obtained when the interbasin transfer objective is given a null weighting while the agricultural demand objective is given more weight than the ecosystem need objective. River managers and decision makers may select feasible operation strategies for the proposed Laonung diversion weir based on their preferences and the results presented in this work.

REFERENCES

Atiem IA, Harmancioglu NB. 2006. Assessment of regional floods using *L*-moments: the case of the River Nile. *Water Resources Management* **20**: 723–747.

Cunnane C. 1988. Methods and merits of regional flood frequency analysis. *Journal of Hydrology* **100**: 269–290.

Dalrymple T. 1960. *Flood Frequency Analyses*, U.S. Geological Survey Water Supply Paper, 1543-A.

Fowler HJ, Kilsby CG. 2003. A regional frequency analysis of United Kingdom extreme rainfall from 1961 to 2000. *International Journal of Climatology* **23**: 1313–1334.

Groupe de recherché en hydrologie statistique (GREHYS). 1996. Presentation and review of some methods for regional flood frequency analysis. *Journal of Hydrology* **186**: 63–84.

Haupt RL, Haupt SE. 2004. *Practical Genetic Algorithms.* John Wiley: Hoboken, NJ.

Hosking JRM. 1990. L-moments: analysis and estimation of distribution using linear combinations of order statistics. *Journal of the Royal Statistical Society, Series B* **52**: 105–124.

Hosking JRM, Wallis JR. 1993. Some statistics useful in regional frequency analysis. *Water Resources Research* **29**: 271–281.

Hosking JRM, Wallis JR. 1997. *Regional Frequency Analysis: An Approach Based on L-Moments.* Cambridge University Press: New York, NY.

Kjeldsen TR, Smithers JC, Schulze RE. 2002. Regional flood frequency analysis in the KwaZulu-Natal province, South Africa, using the index-flood method. *Journal of Hydrology* **255**: 194–211.

Kumar R, Chatterjee C. 2005. Regional flood frequency analysis using L-moments for north Brahmaputra region of India. *Journal of Hydrologic Engineering* **10**: 1–7.

Lim YH, Lye LM. 2003. Regional flood estimation for ungauged basins in Sarawak, Malaysia. *Hydrological Science Journal* **48**: 79–94.

Madsen H, Pearson CP, Rosbjerg D. 1997. Comparison of annual maximum series and partial duration series methods for modeling extreme hydrologic events, 2. Regional modeling. *Water Resources Research* **33**: 759–769.

Norbiato D, Borga M, Sangati M, Zanon F. 2007. Regional frequency analysis of extreme precipitation in the eastern Italian Alps and the August 29, 2003 flash flood. *Journal of Hydrology* **345**: 149–166.

Olden JD, Poff NL. 2003. Redundancy and the choice of hydrologic indices for characterizing streamflow regimes. *River Research and Applications* **19**: 101–121.

Parida BP, Kachroo RK, Shrestha DB. 1998. Regional flood frequency analysis of Mahi-Sabarmati Basin (subzone 3-a) using index flood procedure with L-moments. *Water Resources Management* **12**: 1–12.

Poff NL, Allan JD, Bain MB, Karr JR, Prestegaard BD, Richter BD, Sparks RE, Stromberg JC. 1997. The natural flow regime: a paradigm for river conservation and restoration. *Bioscience* **47**: 769–784.

Richter BD, Baumgartner JV, Powell J, Braun DP. 1996. A method for assessing hydrologic alteration within ecosystems. *Conservation Biology* **10**: 1163–1174.

Richter BD, Baumgartner JV, Wigington R, Braun DP. 1997. How much water does a river need. *Freshwater Biology* **37**: 231–249.

DOI: 10.1002/rra

Shiau JT, Wu FC. 2004a. Assessment of hydrologic alterations caused by Chi-Chi diversion weir in Chou-Shui Creek, Taiwan: opportunities for restoring natural flow conditions. *River Research and Applications* **20**: 401–412.
Shiau JT, Wu FC. 2004b. Feasible diversion and instream flow release using range of variability approach. *Journal of Water Resources Planning and Management* **130**: 395–404.
Shiau JT, Wu FC. 2006. Compromise programming methodology for determining instream flow under multiobjective water allocation criteria. *Journal of the American Water Resources Association* **42**: 1179–1191.
Shiau JT, Wu FC. 2007a. A dynamic corridor-searching algorithm to seek time-varying instream flow releases for optimal weir operation: comparing three indices of overall hydrologic alteration. *River Research and Applications* **23**: 35–53.
Shiau JT, Wu FC. 2007b. Pareto-optimal solutions for environmental flow schemes incorporating the intra-annual and interannual variability of the natural flow regime. *Water Resources Research* **43**: W06433. doi:10.1029/2006WR005523
Shiau JT, Wu FC. 2008. A histogram matching approach for assessment of flow regime alteration: application to environmental flow optimization. *River Research and Applications* **24**: published online. 914–928.
Sivapalan M. 2003. Prediction in ungauged basins: a grand challenge for theoretical hydrology. *Hydrological Processes* **17**: 3163–3170.
Smithers JC, Schulze RE. 2001. A methodology for the estimation of short duration design storms in South Africa using a regional approach based on L-moments. *Journal of Hydrology* **241**: 42–52.
The Nature Conservancy. 2005. *IHA Applications Database*. http://www.nature.org/initiatives/freshwater/files/iha_apps.pdf
Trefry CM, Watkins DW Jr, Johnson D. 2005. Regional rainfall frequency analysis for the state of Michigan. *Journal of Hydrologic Engineering* **10**: 437–449.
Water Resources Agency (WRA). 2003. *Tsengwen Reservoir Transbasin Diversion Project Environmental Impact Assessment*. GPN: 1009200683, Taichung, Taiwan (in Chinese).
Zhang J, Hall MJ. 2004. Regional flood frequency analysis for the Gan-Ming river basin in China. *Journal of Hydrology* **296**: 98–117.

APPENDIX

1. Generalized logistic distribution (GLO)

$$F(\overline{x}) = \frac{1}{1 + \left[1 - \frac{k(\overline{x}-\xi)}{\alpha}\right]^{\frac{1}{k}}} \tag{A.1}$$

where $\overline{x}$ = non-dimensionalized data; ξ, α and k are parameters.

2. Generalized extreme-value distribution (GEV)

$$F(\overline{x}) = \exp\left\{-\left[1 - \frac{k(\overline{x}-\xi)}{\alpha}\right]^{\frac{1}{k}}\right\} \tag{A.2}$$

where ξ, α and k are parameters.

3. Three-parameter lognormal distribution (LN3)

$$F(\overline{x}) = \Phi\left(\frac{\ln(\overline{x}-\zeta)-\eta}{\sigma}\right) \tag{A.3}$$

where ζ, η, and σ are parameters; Φ = standard normal cdf.

4. Pearson type III distribution (PE3)

$$F(\overline{x}) = G\left(\frac{\overline{x}-\eta+\frac{2\sigma}{\gamma}}{\left|\frac{1}{2}\sigma\gamma\right|}, \frac{4}{\gamma^2}\right) \tag{A.4}$$

where η, σ and γ are parameters; G = incomplete gamma function.

5. Generalized Pareto distribution (GPA)

$$F(\overline{x}) = 1 - \left[1 - \frac{k(\overline{x}-\xi)}{\alpha}\right]^{\frac{1}{k}} \tag{A.5}$$

where ξ, α and k are parameters.

DOI: 10.1002/rra